Marine Chemistry 182 (2016) 14–24

Contents lists available at ScienceDirect

Marine Chemistry

journal homepage: www.elsevier.com/locate/marchem

Spatiotemporal variability of nitrous oxide in a large eutrophic estuarine system: The Pearl River Estuary, China

Hua Lin, Minhan Dai *, Shuh-Ji Kao, Lifang Wang, Elliott Roberts, Jin-Yu Terence Yang, Tao Huang, Biyan He

State Key Laboratory of Marine Environmental Science, Xiamen University, Xiamen 361005, China

ARTICLE INFO

Article history:
Received 26 April 2015
Received in revised form 23 January 2016
Accepted 24 March 2016
Available online 11 April 2016

Keywords:
Pearl River Estuary
N_2O
N_2O flux
Spatiotemporal variation
Nitrification

ABSTRACT

The spatiotemporal variations of nitrous oxide (N_2O) in the Pearl River Estuary, a large perturbed estuary, were investigated via six cruises covering both wet and dry seasons during 2007–2011. Significant spatial and temporal variabilities in N_2O concentrations and N_2O saturations were detected. Spatially, N_2O was oversaturated in the entire estuary; ranging from 328 nmol L^{-1}, or 38 times saturation in the O_2-depleted Upper Estuary, down to 11–79 nmol L^{-1} in the Middle Estuary (163–905% saturation), and to ~7 nmol L^{-1} (slight supersaturation) in the Lower Estuary. Temporally, increased N_2O up to 182 ± 82 nmol L^{-1} (1800 ± 750% saturation) was observed in the Upper Estuary during winter at low river discharge in comparison to 76 ± 19 nmol L^{-1} (1163 ± 287% saturation) in summer at high river discharge; whereas no significant seasonal difference was detected within the Middle and Lower Estuaries. The N_2O fluxes decreased by 2 orders of magnitude from upstream to downstream (733 to lower than 5 μmol m^{-2} d^{-1}). Seasonally, the higher N_2O fluxes integrated across the estuary were in spring and winter, and lower fluxes were exhibited in summer and autumn. The annual water–air N_2O flux was estimated to be 37 ± 15 μmol m^{-2} d^{-1}. This rendered a total emission of (1.67 ± 0.89) × 10^9 g N_2O yr^{-1}, which is equivalent to the revised total emission from 19 European inner estuaries (1.35 × 10^9 g N_2O yr^{-1}). Moreover, this amount of N_2O emission equals approximately 30% of reported CO_2 emission from the Pearl River Estuary in terms of greenhouse warming potential. The N_2O production was predominantly modulated by nitrification in the Upper Estuary while in the Middle and Lower Estuaries, estuarine mixing appeared to dominate the N_2O behavior.

© 2016 Elsevier B.V. All rights reserved.

1. Introduction

Nitrous oxide (N_2O), a trace gas with a 114 year lifespan in the atmosphere, has about 300 times greater greenhouse potential relative to CO_2. It is increasing in concentration at a rate of ~0.25% annually due to increasing human activities (IPCC, 2007). Additionally, N_2O contributes to the destruction of stratospheric ozone (Ravishankara et al., 2009), and thus is an important gas component of the earth's climatic system (Bange, 2000).

N_2O is generated as a by-product from the first step of microbial nitrification, i.e. the oxidation of ammonium (NH_4^+) to nitrite (NO_2^-) (Dore and Karl, 1996; Yoshinari et al., 1997; Middelburg and Nieuwenhuize., 2000). N_2O is also known to be produced as an intermediate from denitrification, i.e., the reduction of nitrate (NO_3^-) to N_2 (Naqvi et al., 2000; Walter et al., 2006; Yamagishi et al., 2007). Nitrification is principally autotrophic, whereas denitrification is heterotrophic. Both processes can occur either in the water column or sediments (Codispoti et al., 2001; Bange, 2008). In each case, the N_2O yield is believed to be highly dependent on the ambient dissolved O_2 concentration in aquatic systems (Goreau et al., 1980; Codispoti et al., 2001; Naqvi et al., 2010). N_2O production would be significantly enhanced under low O_2 concentrations (Dai et al., 2008; Codispoti, 2010; Naqvi et al., 2010; Kim et al., 2013).

Marine waters are generally believed to be a major natural and anthropogenic source of atmospheric N_2O (Seitzinger et al., 2000). Coastal aquatic systems, including estuaries, are an important component of the marine N_2O cycle. However, N_2O emissions from estuaries demonstrate considerable uncertainty (Bange et al., 1996; Bange, 2006; Nevison et al., 2003; Barnes and Upstill-Goddard, 2011) due to major spatiotemporal variability and the limited data available. In addition, most early estimates of estuarine N_2O emissions focused on relative small European estuaries (Bange et al., 1996; Bange, 2006; Barnes and Upstill-Goddard, 2011). Mounting evidence suggests that substantial differences occur in different estuarine systems, and the large Asian estuaries might hold an increasingly important role in budgeting the future global N_2O emission with increasing anthropogenic stress (Zhang et al., 2010; Rao and Sarma, 2013). Even within a single estuary, large spatiotemporal variations are present (Harley et al., 2015). This poses a big challenge to reliably constrain the estuarine N_2O effluxes at a global scale.

The Pearl River (Zhujiang) Estuary is a large subtropical Asian estuary altered significantly by human-induced perturbation (Dai et al.,

* Corresponding author.
E-mail address: mdai@xmu.edu.cn (M. Dai).

http://dx.doi.org/10.1016/j.marchem.2016.03.005
0304-4203/© 2016 Elsevier B.V. All rights reserved.

2006, 2008, 2014; He et al., 2014). This estuary is located in one of the most rapidly developing areas of the world during the past three decades. The estuarine environment was greatly affected by the rapid economic growth and anthropogenic stress from cities such as Guangzhou, Hong Kong, Macau, Shenzhen, and Zhuhai. Many environmental issues, such as ammonium contamination and hypoxia, have emerged (Zhai et al., 2005; Dai et al., 2006, 2008; Guo et al., 2009; He et al., 2014). This coupled high-nitrogen and low-oxygen system permits an opportunity to examine nitrogen transformation and the production of N_2O.

We conducted six cruises during 2007–2011 to constrain the water–air N_2O fluxes from the Pearl River Estuary that encompasses both spatial and temporal variations. An estimate of N_2O effluxes into the atmosphere was conducted based on the seasonal and zonal distributions of N_2O distribution. These fluxes and emissions were compared with other estuaries in Asia and Europe. Factors regulating N_2O production were discussed as well.

2. Material and methods

2.1. Study area

The Pearl River is the second largest river in China in terms of annual water discharge (3.26×10^{11} m^3 yr^{-1}). It spans for 2214 km, and drains an area of 452,000 km^2 (Dai et al., 2014). The Pearl River has three main tributaries (Fig. 1); namely, the Xijiang (West River), Beijiang (North River), and Dongjiang (East River). Amongst them, the West River accounts for ~70% of the total freshwater discharge (China Bureau of Hydrology, Ministry of Water Resources, http://sqqx.hydroinfo.gov.cn/websq/). The water discharge rate shows significant seasonality, and ~80% of the discharge takes place in the wet season from April to September (Fig. 2). During winter, the monthly average river discharge is around 2000 m^3 s^{-1}. In contrast, the monthly average water flow rate during the summer can be 8 times higher; peaking at approximately 16,000 m^3 s^{-1} in June.

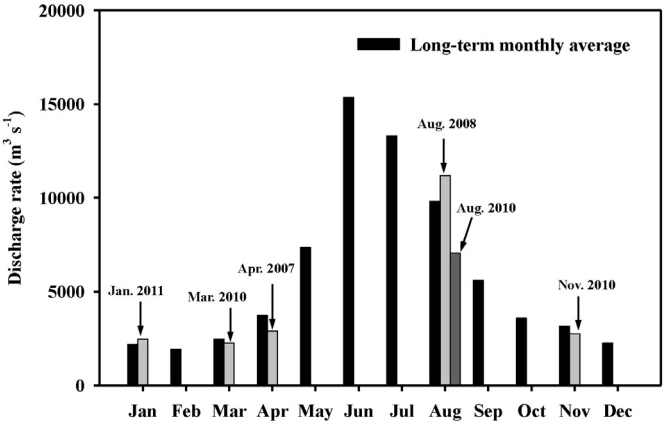

Fig. 2. Long-term monthly averaged water discharge from 2000 to 2011 at the Wuzhou hydrological station on the West River (China Bureau of Hydrology, Ministry of Water Resources, http://sqqx.hydroinfo.gov.cn/websq/). The monthly averaged discharge of survey cruises in April 2007, August 2008, March 2010, August 2010, November 2010, and January 2011 is also shown.

For the convenience of N_2O flux estimation, we divided the survey region (with a total area of ~2789 km^2) into 3 zones in accordance to the N_2O level and the geometry of the estuary similar to Guo et al. (2009) (Fig. 1). These 3 zones are (1) Upper Estuary: Guangzhou section, the channel flowing through the city of Guangzhou to Humen Outlet, with a length of ~75 km and an area of ~107 km^2; (2) Middle Estuary: Inner Lingdingyang, from Humen Outlet to Inner Lingding Island, with a length of ~40 km and an area of ~582 km^2; (3) Lower Estuary: Outer Lingdingyang, from Inner Lingding Island to the Outer Estuary, with a length of ~50 km and an area of ~2100 km^2 (Fig. 1, Table 1).

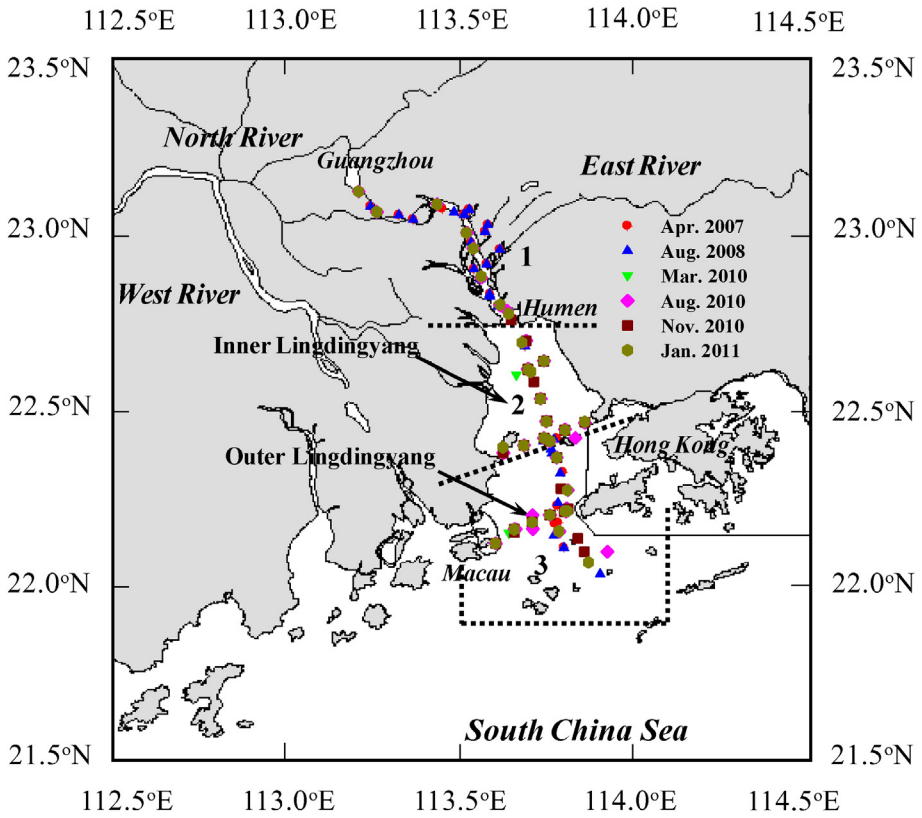

Fig. 1. Map of the Pearl River Estuary showing the sampling sites during 2007–2011. This study partitioned the estuary into 3 zones: (1) Upper Estuary (Humen upstream); (2) Middle Estuary (Inner Lingdingyang); (3) Lower Estuary (Outer Lingdingyang and beyond).

Table 1
Surface water N_2O and N_2O flux in the Pearl River Estuary. The study area was divided into 3 zones: (1) Upper Estuary; (2) Middle Estuary; (3) Outer Estuary.

				Area	N_2O (nmol L^{-1})				N_2O saturation (%)				N_2O flux (μmol m^{-2} d^{-1})[a]				N_2O emission (10^3 mol d^{-1})[b]	
Season	Survey	Zone	N	(km^2)	Ave	SD	Max	Min	Ave	SD	Max	Min	Ave	SD	Max	Min	Ave	SD
Spring	Apr 2007	1	23	107	152	42	232	87	1909	529	2884	1071	316	92	485	171	34	10
		2	6	582	33	17	66	19	439	206	849	274	55	36	127	27	32	21
		3	6	2100	13	7	27	7	197	109	383	106	14	17	44	1	30	35
	Mar 2010	1	7	107	151	104	329	55	1920	1217	3799	674	310	209	637	115	33	22
		2	13	582	22	11	49	11	272	130	614	255	31	26	95	7	18	15
		3	9	2100	10	2	12	8	129	17	231	112	3	1	5	2	6	2
Summer	Aug 2008	1	24	107	72	56	276	31	1103	908	3229	430	177	161	733	58	19	17
		2	8	582	19	6	26	11	275	80.1	380	163	30	14	47	11	18	8
		3	7	2100	12	5	20	6	186	76	300	101	14	13	33	0.1	30	27
	Aug 2010	1	7	107	76	19	97	44	1163	287	1477	676	175	47	227	95	19	5
		2	13	582	26	13	57	15	399	197	905	232	48	33	134	20	28	19
		3	10	2100	11	2	13	8	171	24	200	138	10	5	17	0.1	21	10
Autumn	Nov 2010	1	0	107	ND	ND	ND	ND	ND	ND	ND	ND	ND	ND	ND	ND	ND	ND
		2	13	582	25	12	66	16	327	150	851	227	33	23	115	17	19	13
		3	10	2100	11	3	15	9	153	31	209	124	7	4	16	3	15	9
Winter	Jan 2011	1	7	107	182	82	283	83	1800	750	2740	881	330	152	519	144	35	16
		2	13	582	34	19	79	16	384	204	886	187	50	38	139	15	29	22
		3	10	2100	15	4	20	9	180	44	241	115	13	7	23	2	28	16

ND represents non-detectable
[a] Average N_2O flux is 37 ± 15 μmol m^{-2} d^{-1}.
[b] Annual N_2O emission is $(3.8 \pm 2.0) \times 10^7$ mol yr^{-1}.

2.2. Sampling and analysis

2.2.1. Water sampling

Water samples were collected during six cruises (April 2007, August 2008, March 2010, August 2010, November 2010, and January 2011). For the convenience of discussion hereafter: April 2007 and March 2010 are regarded as spring cruises; August 2008 and August 2010 as summer cruises; November 2010 as the autumn cruise; January 2011 as the winter cruise. Samples were taken along a main north to south transect as shown in Fig. 1. Discrete sampling locations were based on the salinity gradient (every ~3 PSU) within the estuarine mixing zone, and by distance (every 5–10 km) when no salinity changes occurred upstream of Humen. In addition, water samples along two transects crossing from west to east were also taken in the Middle and Lower Estuaries during four cruises from 2010 to 2011. Water samples for N_2O, nutrients and dissolved oxygen (DO) were collected at 0.5 m below the surface using Go-Flo bottles.

2.2.2. Analysis of N_2O

Samples for dissolved N_2O were immediately taken in 100 mL glass flasks, poisoned with 100 μL saturated $HgCl_2$ solution and stoppered with a rubber septum without any headspace gas. The samples were stored in the dark at 4 °C prior to laboratory analysis. Sample analysis was performed within one month after collection.

Our experiments demonstrated no significant differences in dissolved N_2O concentrations from replicate samples ($n = 12$) analyzed after two months storage. The dissolved N_2O concentrations were measured at State Key Laboratory of Marine Environmental Science (MEL), Xiamen University. The analytical method was a modification of the method described by Chen et al. (2007). A purge and trap system (Tekmar Velocity XPT) coupled with a gas chromatograph was set up, with the analytical procedure as the following: the water sample of 5 mL volume was transferred to the glass purge vessel, where the sample was purged with a 20 mL min^{-1} nitrogen gas flow of ultra-high purity (99.999%) for 10 min. The displaced gas was transferred to a purge trap (24 cm molecular sieve 5 A, mesh 80/100) at room temperature. During desorption (250 °C for 2 min) gases collected in the trap were transferred through a heated transfer line to the GC injector port. Gas chromatographic analyses were performed with a Hewlett-Packard Model 6890 equipped with a micro-electron capture detector (μECD) operating at 300 °C. Chromatographic separation was achieved on a RT-Q Plot wide-bore column (30 m × 0.53 mm I.D., $d_f = 20$ μm) (Restek). The column temperature was held at 50 °C. A 5% mixture gas of CH_4–Ar at a flow rate of 5 mL min^{-1}, and 20 mL min^{-1} was used as carrier gas and make-up gas. Calibration of N_2O concentrations was calculated from the peak areas with standard gases of 1.0 and 5.0 ppmv N_2O/N_2 (Research Institute of China National Standard Materials). Certain volumes of standard gas were transferred into the glass purge vessel and subsequently analyzed by the same procedure used for water samples. When many water samples were analyzed standards were included every 5–10 samples. The precision of this method was estimated to be better than ±5%.

2.2.3. Ancillary measurements

Temperature and salinity were measured continuously using an YSI multi-parameter meter fitted in the under-way measurement system described in Zhai et al. (2005) and Dai et al. (2006). Discrete DO was measured on board using the Winkler titration method.

Nutrients samples were stored at −20 °C until analysis except for NH_4^+, which was analyzed on board with the indophenol blue spectrophotometer method (Pai et al., 2001). NO_2^- and NO_3^- measurements were processed at Xiamen University, using classic colorimetric methods with a Technicon AA3 Auto-Analyzer (Blan-Lube). Nutrient sample analysis was performed within one month after collection. Nitrification rates were measured using an inhibitor technique. Both methods were described in Dai et al. (2008).

DO and nutrient data from April 2007 and August 2008 were cited from Guo et al. (2009), He et al. (2010), and He et al. (2014). The nitrification rates data in April 2007 and August 2008 were cited from He et al. (2014). The parameters observed in March 2010, August 2010, November 2010, and January 2011 were new observations.

2.3. Calculations

The excess N_2O (ΔN_2O) was estimated as the difference between the calculated N_2O equilibrium concentration and the measured concentration of N_2O as the following equation;

$$\Delta N_2O \left(\text{nmol L}^{-1}\right) = N_2O\_\text{observed} - N_2O\_\text{equilibrium} \quad (1)$$

where N_2O_observed is the N_2O concentration measured in the water, and N_2O_equilibrium is the N_2O concentration at relative equilibrium

with atmospheric concentration. The equilibrium values of N_2O were calculated with the equation given by Weiss and Price (1980). Atmospheric N_2O was not measured during these cruises. Global mean atmospheric N_2O mixing ratios of 320 ppb for 2007, 321 ppb for 2008, and 323 ppb for 2010 from the NOAA/ESRL halocarbons in situ program (http://www.esrl.noaa.gov/gmd) were used for the calculations in this study.

The N_2O flux through the air–sea interface was estimated based on Eq. (2);

$$F = k \times \Delta N_2O \quad (2)$$

where F ($\mu mol\ m^{-2}\ d^{-1}$) is the flux across the air–sea interface, and k ($cm\ h^{-1}$) is the gas transfer velocity depending on wind and water temperatures.

k was calculated using the Borges et al. (2004) equation:

$$k = 0.31 \times (9.7 + 3.64 \cdot u_{10}) \times (Sc/600)^{-0.5} \quad (3)$$

where U_{10} is the wind speed at 10 m above the water surface. Sc is the Schmidt number calculated from temperature, which is the relationship between viscosity and the diffusion coefficient of N_2O in water that depends on the water temperature and salinity (Wanninkhof, 1992). In our study, S < 30 was treated as freshwater, while S > 30 was treated as seawater. The monthly average wind speeds obtained from Hong Kong Observatory (http://www.weather.gov.hk/cis/region_climat/CCH/CCH_mean_e.htm) from the meteorological station located at the estuary mouth were used for the calculation of the water–air N_2O fluxes.

As previously stated, the estuary was divided into 3 zones: Upper Estuary, Middle Estuary, and Lower Estuary. Each zone area was multiplied by the average N_2O fluxes in spring, summer, autumn and winter that was upscaled to give a seasonal emission value for each zone. They were subsequently summed to calculate the yearly emission for the whole estuary and sections of the estuary.

2.4. Statistical analysis

Significant differences of concentrations, saturations and fluxes in different zones and seasons were tested with t-tests. All statistical analyses were conducted in SPSS with a significance level of $p < 0.05$.

3. Results

3.1. Hydrochemistry

Freshwater discharge rates from the Pearl River system showed significant seasonal variations. Higher values were demonstrated in the

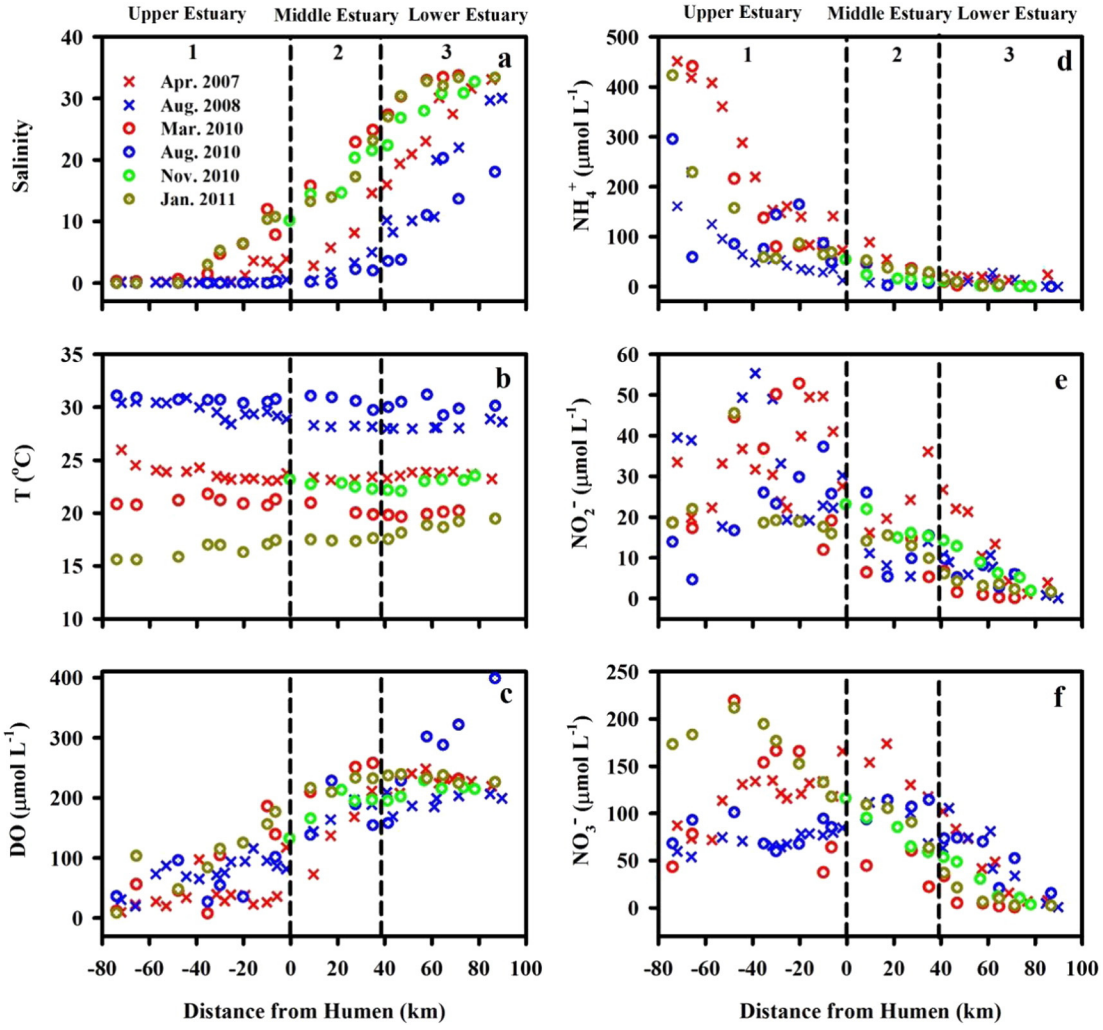

Fig. 3. Spatial distributions of salinity (a), temperature (b), DO (c), NH_4^+ (d), NO_2^- (e), and NO_3^- (f) in the Pearl River Estuary based on six cruises (April 2007, August 2008, March 2010, August 2010, November 2010, and January 2011). The distance is positive for downstream and negative for upstream of the Humen Outlets. Black lines separate distinct reaches: Reach (1) Upper Estuary (Humen upstream); Reach (2) Middle Estuary (Inner Lingdingyang); Reach (3) Lower Estuary (Outer Lingdingyang and beyond). The DO and nutrient data for the Apr 2007 cruise were cited from Guo et al. (2009); He et al. (2010); He et al. (2014); and DO and nutrient data for the August 2008 cruise were cited from He et al. (2014).

summer (~13,700 $m^3\ s^{-1}$ in August 2008), and lower values during winter (~2200 $m^3\ s^{-1}$ in January 2011) (Fig. 2). The spatial distribution of salinity within the estuary was largely reflective of different freshwater discharge rates in different seasons. In the vicinity of Humen Outlet, the salinity was ~0–1 in summer (August 2008 and August 2010). In contrast, in winter (January 2011), estuarine mixing moved upstream and salinity of ~12 was exhibited at the Humen Outlet (Fig. 3a). Average salinity in the Middle and Lower Estuaries, demonstrated higher values in winter (~18 and ~29 respectively) than in summer (~5 and ~17, respectively) (Fig. 3a). In spring and autumn (April 2007, March 2010, and November 2010), the salinity distribution pattern was median to summer and winter (Fig. 3a). The surface water temperature ranged from 19.4–24.7 °C (in spring), 27.2–31.2 °C (in summer), 20.9–23.2 °C (in autumn), and 15.6–19.4 °C (in winter) (Fig. 3b).

Pronounced oxygen depletion was observed in the surface water in the Upper Estuary throughout the year (Fig. 3c), which has been reported previously (Dai et al., 2006, 2008; Guo et al., 2009; He et al., 2014). Seasonally, the most severe oxygen depletion of surface DO lower than 63 μmol L^{-1} (2 mg L^{-1}) was detected in the entire upstream of the Humen Outlet during spring. The lowest concentration of 8–12 μmol L^{-1} (~4% DO saturation) was observed in March 2010. In winter, estuarine mixing played a significant role in raising the oxygen content upstream of Humen, and the observed oxygen depletion area was relatively narrow compared to spring. Downstream, DO concentration increased gradually with the salinity gradient, reaching nearly saturated or supersaturated conditions in the Lower Estuary (Fig. 3c). In August 2010, there was a notable maximum oxygen concentration (~400 μmol L^{-1}) that was observed in the Lower Estuary (Fig. 3c) due to high net community production (Guo et al., 2009; He et al., 2014).

Similar distribution patterns and high levels of dissolved inorganic nitrogen (DIN) were detected in the Pearl River Estuary during our survey cruises (Fig. 3d–f). This observation was reported in previous studies (Dai et al., 2008, He et al., 2014). Low-nutrient seawater mixing accounted for the significant seaward-decreasing trend in all nitrogen species. In comparison to winter and spring, larger freshwater dilution and short water residence time may have accounted for the overall lower total DIN in summer.

In all seasons, NH_4^+ was the dominant species of DIN in the Upper Estuary, accounting for ~80% of DIN (Fig. 3d). NH_4^+ concentrations were highest at the freshwater end-member, peaking at ~470 μmol L^{-1} in April 2007. This region was directly impacted by regional wastewater discharge (Dai et al., 2008; He et al., 2014). Slightly downstream, NH_4^+ concentrations rapidly declined in correlation with increasing NO_2^- and NO_3^- concentrations (Fig. 3e and f). This data supported the earlier contention that the upper Pearl River Estuary is a site of permanent and strong NH_4^+ nitrification (Dai et al., 2006, 2008; He et al., 2014). With the chief drop in the Upper Estuary, NH_4^+ concentrations gradually decreased to the detection limit in the seaward direction.

The NO_3^- distribution along the Pearl River Estuary showed a few peaks in the Middle or Upper Estuary (Fig. 3f). Occurrence of those peaks was related to local sewage inputs from major cities. In addition, their locations may have been affected by the tidal motion superimposed by the complex geometry of the Lingdingyang (Dai et al., 2006, 2008; He et al., 2014). The highest NO_3^- value in March 2010 was up to 230 μmol L^{-1}. During all cruises, NO_3^- concentrations gradually decreased in the Lower Estuary, due to dilution with seawater with lower NO_3^- contents (Fig. 3f).

3.2. Spatial and seasonal variations of N_2O concentration and its saturation

The N_2O distribution along the Pearl River Estuary displayed pronounced spatial variability, ranged from 6 to 329 nmol L^{-1} that corresponded to saturations of 101–3800% (Figs. 4 & 5, Table 1). Hence, the Pearl River Estuary was a net source of atmospheric N_2O.

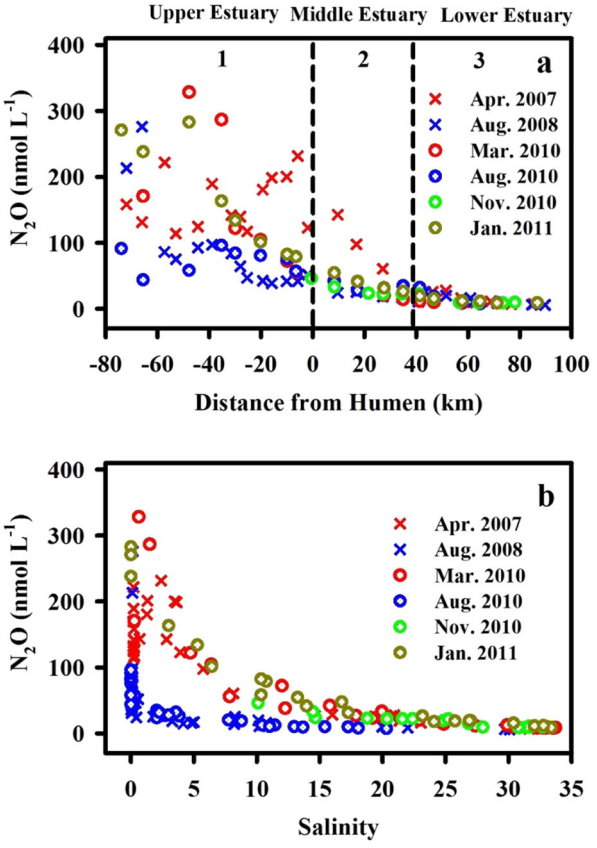

Fig. 4. N_2O vs. distance from Humen (a) and vs. salinity (b) in the Pearl River Estuary.

The general pattern was that N_2O was higher at the Upper Estuary, decreasing downstream during all seasons. Take March 2010 (Figs. 4 and 5c, Table 1) as an example. In the main north to south transect, the Upper Estuary (Zone 1) exhibited very high N_2O (55–329 nmol L^{-1}), which paralleled to saturations of 674–3800%. This level was similarly reported in April 2004 by Xu et al. (2005). N_2O decreased in the Middle Estuary to 11–49 nmol L^{-1} (255–614% saturation). In the Lower Estuary, the N_2O concentration was reduced to about 6 nmol L^{-1}, which is in near-equilibrium with the atmosphere. In two transects crossing from west to east, slightly higher N_2O concentrations were observed in the west compared to the east. Values ranged from 13 to 17 nmol L^{-1} in the Middle Estuary transect, and 8 to 10 nmol L^{-1} in the Lower Estuary transect. These results are inversely proportional to salinity readings. Regarding the N_2O-salinity relationship, N_2O dropped rapidly against salinity from 329 nmol L^{-1} in the Upper Estuary to 55 nmol L^{-1} at ~12–13; progressively decreasing seaward with increasing salinity. Seaward of salinities with values of ~33, N_2O concentrations were close to atmospheric equilibrium (Table 1, Fig. 4b).

Additionally, the seasonal variation was also significant with generally higher N_2O concentrations during winter/spring than summer/autumn. Zonal average N_2O values in different seasons were summarized in Table 1 and further presented in Fig. 6.

In the Upper Estuary (Zone 1), average N_2O was higher in spring (152 ± 42 nmol L^{-1} in April 2007, and 151 ± 104 nmol L^{-1} in March 2010) and winter (182 ± 82 nmol L^{-1} in January 2011), but much lower during summer (72 ± 56 nmol L^{-1} in August 2008, and 76 ± 19 nmol L^{-1} in August 2010). The average N_2O value in the Middle Estuary (Zone 2) and the Lower Estuary (Zone 3) ranged from 19 to 34 nmol L^{-1} and 11 to 15 nmol L^{-1}, respectively (Table 1). The seasonal variation in the Middle and Lower Estuaries displayed no statistical significance compared to Upper Estuary. In the Upper Estuary, the intra-seasonal variation was small both in spring and summer.

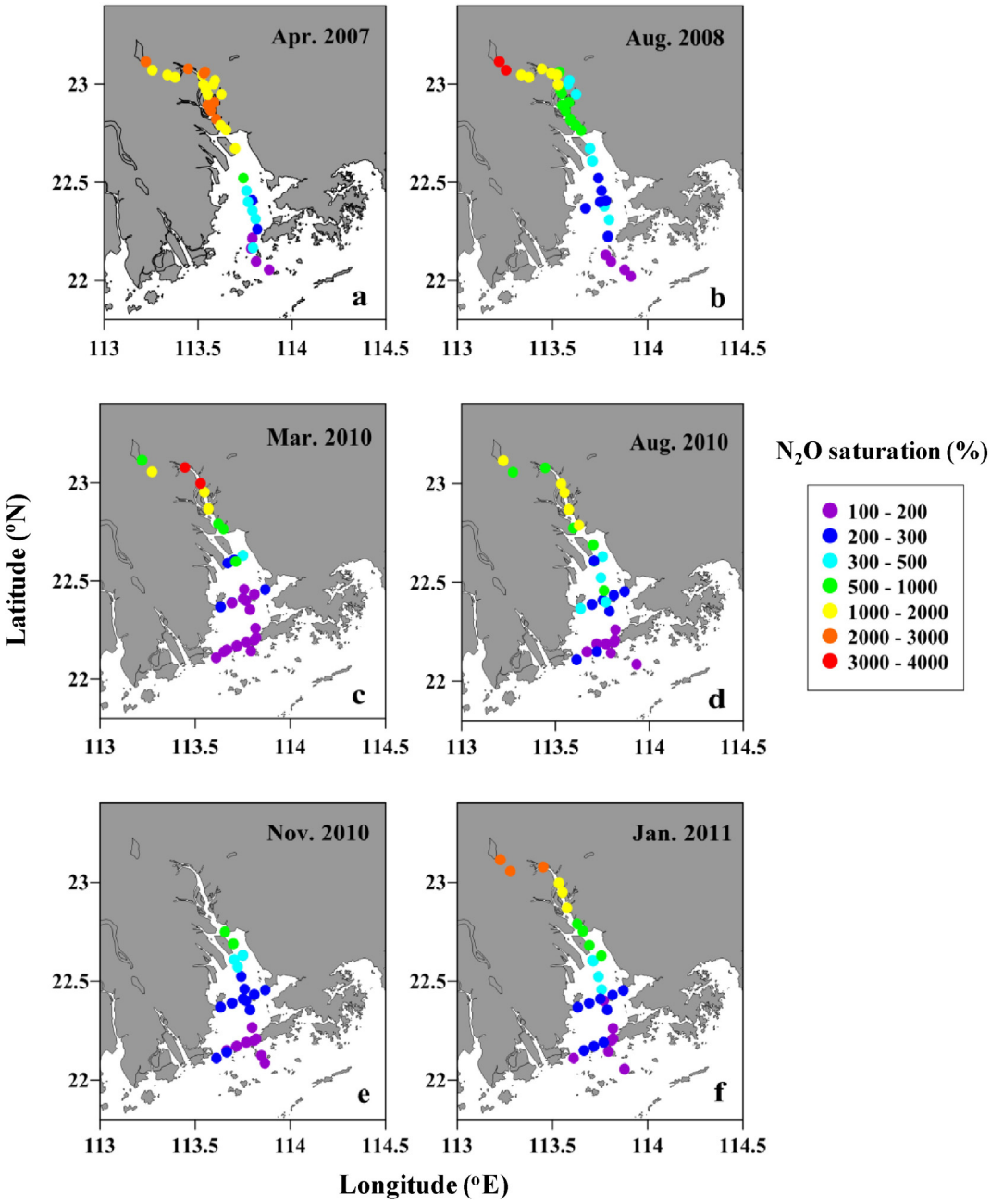

Fig. 5. Spatial distributions of N_2O saturations in the Pearl River Estuary in (a) April 2007, (b) August 2008, (c) March 2010, (d) August 2010, (e) November 2010, and (f) January 2011.

3.3. Spatial and seasonal variations in N_2O fluxes

The monthly average wind speeds, ranging from 4.7 to 5.6 m s^{-1}, were used for the calculation of the N_2O fluxes. Similar to the distribution of N_2O concentration, the water–air N_2O fluxes displayed considerable spatially variability by 2 orders of magnitude in the Pearl River Estuary. The N_2O flux maximum of 733 μmol m^{-2} d^{-1} was observed at the Upper Estuary, while the N_2O flux was reduced to values lower than 5 μmol m^{-2} d^{-1} towards the mouth of the estuary (Fig. 6c, Table 1).

On a seasonal time scale, substantially elevated N_2O fluxes were exhibited during winter (330 ± 152 μmol m^{-2} d^{-1}) and spring (313 ± 150 μmol m^{-2} d^{-1}) in Upper Estuary than in summer (176 ± 106 μmol m^{-2} d^{-1}) (Fig. 6c). The intra-seasonal variation in the N_2O fluxes was generally low both in summer and spring. The annual average N_2O flux from entire Pearl River Estuary was estimated to be 37 ± 15 μmol m^{-2} d^{-1}.

4. Discussions

4.1. Factors influencing N_2O distribution

Factors contributing to the variations of N_2O in an estuarine system include its production primarily via nitrification that is related to the substrate level (NH_4^+ and NO_2^-) and its ambient environment; notably, DO and physical conditions such as river discharge, estuarine mixing and outgassing. Besides nitrification, denitrification may also produce or consume N_2O. In this section, we discuss the main factors modulating the N_2O distribution in the Pearl River Estuary. The Upper Estuary was characterized by strong nitrification fueled by high NH_4^+ under oxygen

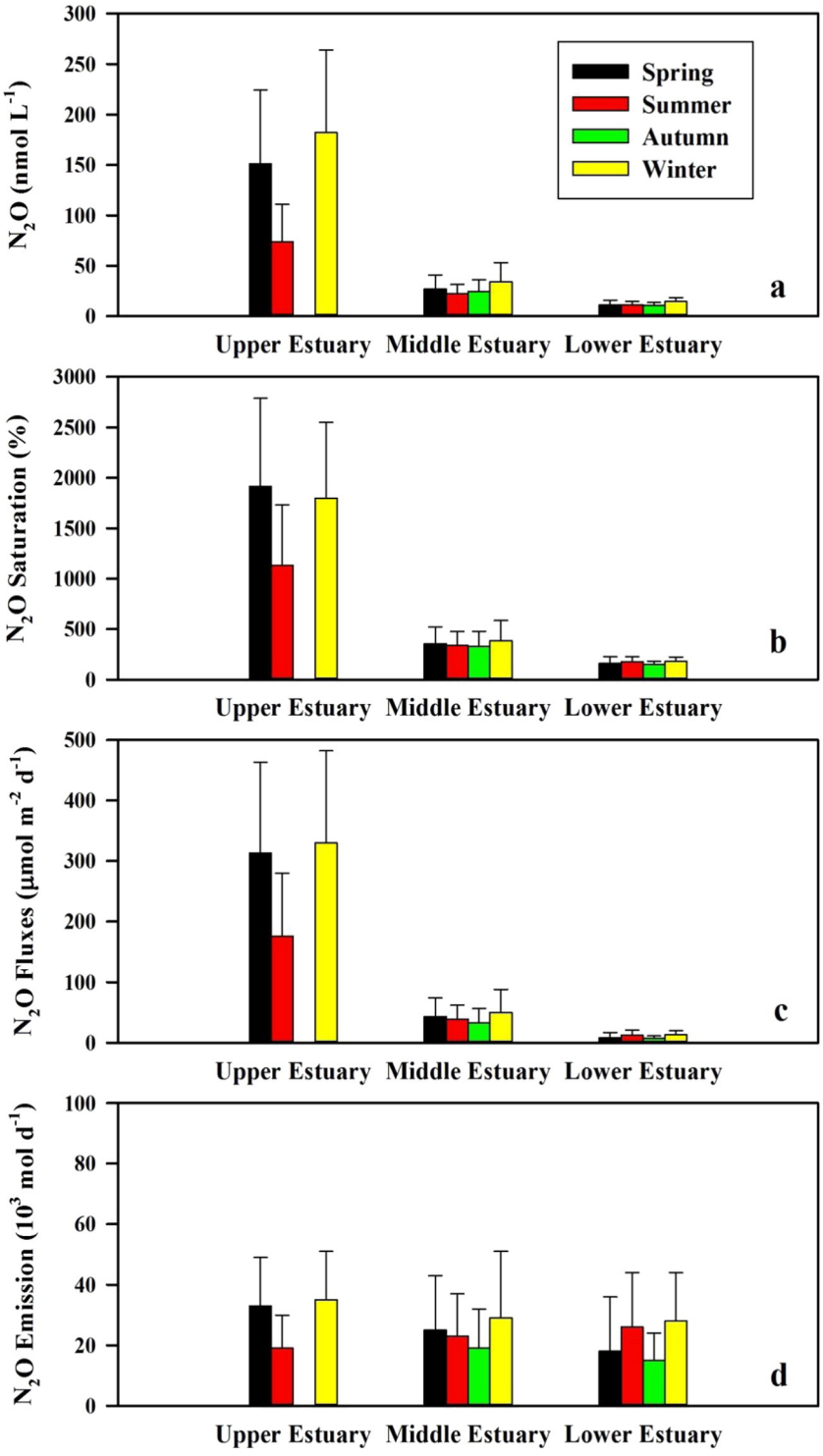

Fig. 6. Zonal average of surface water N_2O concentration (a), saturation (b), fluxes (c), and emissions (d) from the Pearl River Estuary.

depleted conditions, while the Middle and Lower Estuaries were featured by estuarine mixing that played a major role in modulating the N_2O variability.

4.1.1. Upper Estuary

As shown, the Upper Estuary featured very high concentrations of N_2O, NH_4^+, DIN levels (Dai et al., 2006, 2008). Fig. 7 further demonstrated that excess N_2O (ΔN_2O) exhibited positive correlations with nitrogen loading (NH_4^+ and DIN) in the Pearl River Estuary, indicating the significance of nitrification as observed in other eutrophic estuaries (Abril et al., 2000; de Wilde and de Bie, 2000; Garnier et al., 2006). High N_2O production in the Upper Estuary would be attributed to high NH_4^+ effluence (Fig. 7a). This validated that nitrification was the possible mechanism for N_2O production. Barnes and Upstill-Goddard (2011) similarly reported high N_2O production in the Tees and Tyne estuaries in UK, which was a nitrification product of NH_4^+ derived from wastewater inputs.

As Fig. 8 showed, the nitrification rates were high in the surface waters of the upper Pearl River Estuary; with an ammonia oxidation rate of 8.8–22.8 μmol N L^{-1} d^{-1} in April 2007, and from below the detection limit to 27.0 μmol N L^{-1} d^{-1} during August 2008 (He et al., 2014).

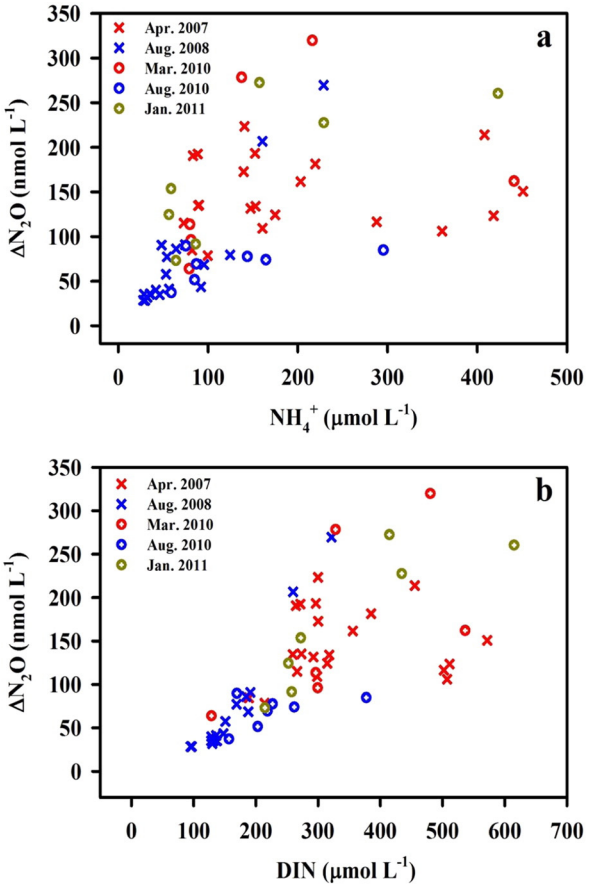

Fig. 7. Relationships between excess N_2O (ΔN_2O) with NH_4^+ (a) and DIN (b) in the upper of Pearl River Estuary.

These reports suggest a strong presence of nitrification in the Upper Estuary. The high abundance of ammonium oxidizing bacteria was also quantified in the prior study (Dai et al., 2008). The concentration of nitrifier bacteria within the water column of Pearl River Estuary was between 2 and 3500 cells mL^{-1}. The highest densities occurred at the Upper Estuary, and dramatically decreased with increasing salinity. The distribution pattern of nitrifier abundance was broadly consistent with nitrification rates (Dai et al., 2008). N_2O production was in agreement with the pattern of NH_4^+ oxidation rates. Both showed higher reading upstream, with values decreasing seaward (Fig. 8). This pattern

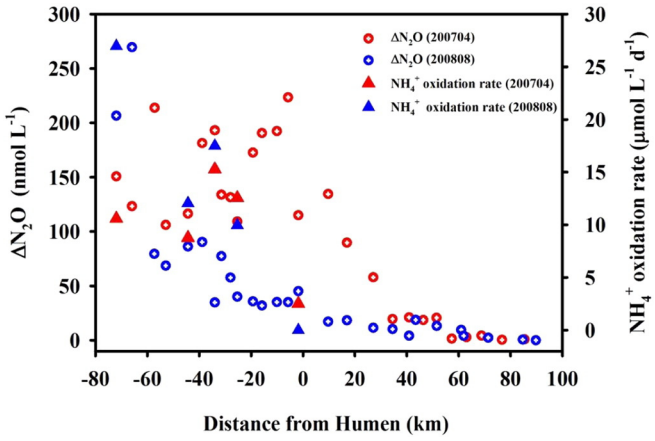

Fig. 8. Relationships between excess N_2O (ΔN_2O) with NH_4^+ oxidation rate in the Pearl River Estuary. The NH_4^+ oxidation rate data for the April 2007 and August 2008 cruise were cited from He et al. (2014).

implied that ammonium oxidation was an important N_2O source in the water column.

It is known that low dissolved O_2 favors nitrification, and subsequently N_2O production (Kim et al., 2013). The upper Pearl River Estuary was severely depleted in O_2 (Dai et al., 2006, 2008; He et al., 2014). The gradient of oxygen depletion ($\Delta O_2 = [O_2]_{eq} - [O_2]$) along the estuary impacted the occurrence and intensity of nitrification, which additionally impacted the N_2O production (Codispoti, 2010; Kim et al., 2013). The relationships between ΔN_2O and ΔDO showed positive correlation during all seasons, with high N_2O emerging at low DO concentrations (Fig. 9). This pattern was similar with previous studies reported in other estuaries (McElroy et al., 1978; De Wilde and De Bie, 2000) and ocean margins (Cohen and Gordon, 1979; Patra et al., 1999; Walter et al., 2006; Löscher et al., 2012).

The N_2O concentration in the Upper Estuary showed remarkable seasonal variations. Significantly higher fresh water discharge in summer (13,700 $m^3\ s^{-1}$) than in winter (2200 $m^3\ s^{-1}$) would significantly dilute both the N_2O and its substrate such as DIN. In addition, the water residence time of Upper Estuary in summer (~3 days) was lower than that in winter (~5 days). Longer residence time benefits N_2O accumulation. In fact, the water column N_2O production rate of 30 nmol N $L^{-1}\ d^{-1}$ can be derived by assuming an ammonium oxidation rate of 20 μmol N $L^{-1}\ d^{-1}$ and the yield of the N_2O during nitrification of 1.5‰ (Elkins et al., 1978; De Wilde and De Bie, 2000). Obviously, the N_2O concentration can be built up to observed levels within a few days without outgassing. The role of denitrification in our study remains unclear although our calculation supports that nitrification was a primary source for water column N_2O.

4.1.2. Middle and Lower Estuaries

In the Middle and Lower Estuaries, N_2O rapidly dropped with increasing salinity (Fig. 4b); indicating that low N_2O seawater was diluting the high N_2O estuarine water. Thus the estuarine mixing process might play an important role in the modulation of N_2O distribution in the Pearl River Estuary. Here, we applied two end-members mixing model between freshwater and seawater to derive the conservative N_2O. This was subsequently compared with the field observations to derive the net alteration of N_2O during the estuarine mixing. Variations of seawater end-members in different seasons were small: 7 nmol L^{-1} for all cruises. However, the variation of the freshwater end-member at the Humen Outlet, where the estuarine mixing initiated for the middle and lower estuarine mixing, was large in different cruises. Different freshwater end-members were used, with higher values in during winter and spring (70–140 nmol L^{-1}) in contrast to summer (~55–75 nmol L^{-1}).

The N_2O difference between the two end-member mixing and observation, denoted here as RN_2O (the model prediction minus field observation), would suggest biogeochemically mediated and/or the outgassing portion of N_2O. The result was shown in Fig. 10a, the

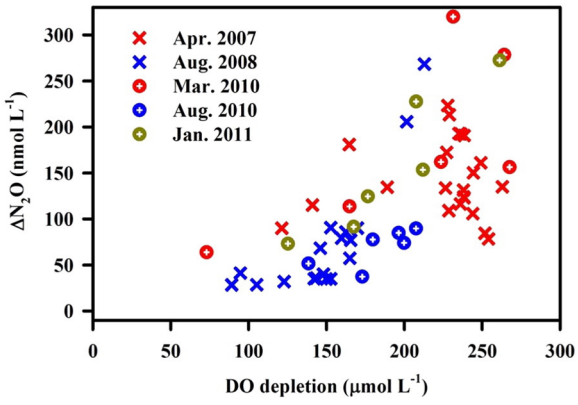

Fig. 9. Excess N_2O (ΔN_2O) vs. oxygen depletion ($\Delta O_2 = [O_2]_{eq} - [O_2]$) plots in the upper Pearl River Estuary.

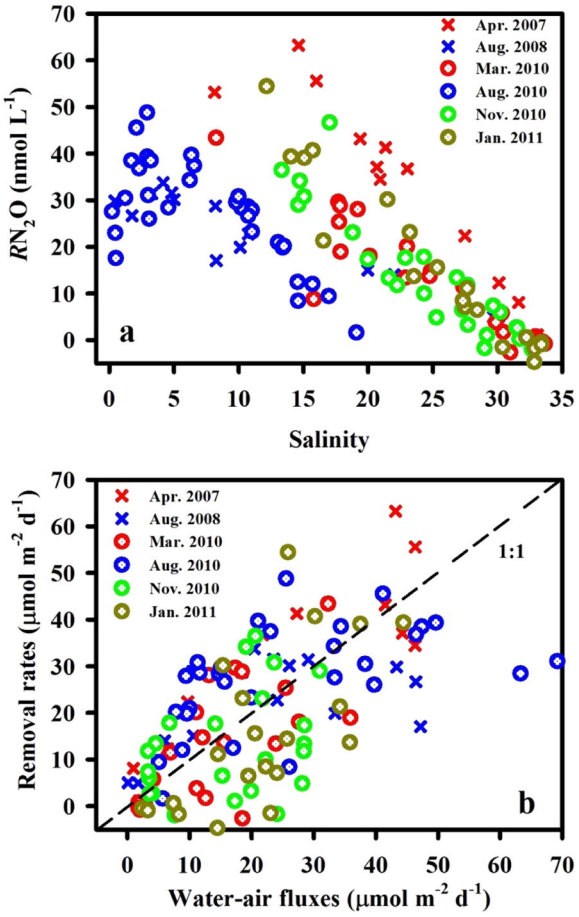

Fig. 10. RN_2O vs. salinity (a) and N_2O removal rates vs. water–air N_2O fluxes (b) in the Pearl River Estuary (Middle- and Lower Estuary). RN_2O (the model prediction minus field observation) represent the removal portion of N_2O during the estuarine mixing.

RN_2O decreased with salinity in all cruises in the Middle and Lower Estuaries. Increased values were observed during winter and spring (0–70 nmol L^{-1}) than in summer (0–50 nmol L^{-1}). This indicated that more N_2O in winter and spring was removed than in summer at the same salinity level. If we assume the water residence time was 3 days in summer and 5 days in other seasons (Wong and Cheung, 2000; Guo et al., 2009), and the average depth of the Lingdingyang sub-estuary was 5 m, we could calculate the N_2O removal rates in the Middle and Lower Estuaries. The N_2O removal rates were compared with the water–air N_2O fluxes (Fig. 10b), in which most were located around the 1:1 line, suggesting that most of the N_2O removal in the water column was released to the atmosphere and in-stream biological processes were not important. Exception for a few stations near Humen Outlet, most of the observational nitrification rates in the Middle and Lower Estuaries were below the detection limit (<0.2 μmol N L^{-1} d^{-1}) (Dai et al., 2008). This represented <1.5 μmol m^{-2} d^{-1} N_2O production by using similar assumption as applied for Upper Estuary, and averaged 5 m depth in the Middle and Lower Estuaries. Compared with outgassing, the contribution from water column nitrification on N_2O was insignificant. In fact, that outgassing largely explained the reduction of N_2O during travel downstream, and also implied that N_2O removal or production from sediment water interface can be neglected.

Consequently, in the Upper Estuary, N_2O production was enhanced under high-DIN loading and high-oxygen depletion condition. Strong nitrification appeared to largely contribute to the high N_2O production. In the Lower and Middle Estuaries, mixing with lower N_2O seawater along with water–air N_2O exchanges was responsible for the variability of N_2O concentrations.

4.2. N_2O emission and comparison with European and other Asian estuaries

Wide spatiotemporal integrated monitoring provided us to obtain reliable N_2O emission from the entire Pearl River Estuary. The annual water–air N_2O emission was estimated to be $(3.8 \pm 2.0) \times 10^7$ mol yr^{-1}. Converting to equivalent greenhouse effect, this emission (1×10^{10} mol CO_2) accounts for approximate ~30% of CO_2 emission (3×10^{10} mol CO_2) in the Pearl River Estuary (Guo et al., 2009).

The uncertainties of N_2O emission estimation in the Pearl River Estuary arise from various sources: scaling errors from the estuary, uncertainties of the transfer velocity versus wind speeds, and bias in mean N_2O values due to the spatial and temporal variances. The errors from area of estuary estimation were believed to be within 5% (Guo et al., 2009; Dai et al., 2014). The transfer velocity versus wind speeds (varied between 4.7 and 5.6 m s^{-1}) carried an error of up to 25%. The uncertainty in estuarine N_2O saturation could be 20% (1σ of the estuarine mean) including the uncertainty in N_2O analysis. Using the individual errors above, the maximum uncertainty in our N_2O emission estimate for the Pearl River Estuary was up to ±54%.

The previous reports for the European and Asian estuaries, N_2O saturation varied over a wide range of 84% to 6506% at various temporal and spatial scales (Table 2). The observed N_2O concentrations in

Table 2
N_2O concentrations, saturations, and fluxes in the European and Asian estuaries.

Estuaries	Date	N_2O concentration (range) (nmol L^{-1})	Mean N_2O saturation (range) (%)	Mean N_2O flux (range) (μmol m^{-2} d^{-1})	References
European					
Schelde	Oct 1978 to Jul 1996	10–338	710 (100 − 3100)	66.6 (0–520)	De Wilde and De Bie (2000)
Gironde	Nov 1991	10–19	132 (106–165)	25.5	Bange et al. (1996)
Loire	Sep 1998	7.3–21	168 (84–271)	14.2	de Bie et al. (2002)
Thames	Feb 1999	15–95	321 (93–681)	69.1	de Bie et al. (2002)
Colne	Aug 2001 to Mar 2002		993	226	Dong et al. (2004)
Humber	Jul 2001 to Oct 2002		396 (157–6506)	76.6	Barnes and Upstill-Goddard (2011)
Elbe	Apr 1997		202 (139–374)	33.6	Barnes and Upstill-Goddard (2011)
Ems	Jun 1997		418 (181–1794)	76.6	Barnes and Upstill-Goddard (2011)
Asian					
Indian estuaries	Jul 2011 to Jan 2012	13.7 (3.5–414)	204 (72–5902)	1.3 (−1.12–14.2)	Rao and Samar (2013)
Adyar	Aug 2003 to Dec 2004	5–82		23.2 (3.6–85.0)	Rajkumar et al. (2008)
Tokyo Bay	May to Oct 1994	8.83–139	400 (116–1630)	30.3 (6.42–107)	Hashimoto et al. (1999)
Yangtze River	2002 to 2006	19.4 (6.04–21.3)	137 (84–363)	15.1	Zhang et al. (2010)
Jiulong River	Jul 2010 to Aug 2011	12.2–113.4	380 (197–1605)	32.2 (4.8–98.0)	Wu et al. (2013)
Pearl River	Sep 2003	20–55			Chen et al. (2008)
Pearl River	Apr 2004,	57–329	674–4134		Xu et al. (2005)
Pearl River	Apr 2007 to Jan 2011	6.0–276	450 (101–3800)	37 (0.1–733)	This study

the upper Pearl River Estuary were comparable to those reported for the Scheldt Estuary, Humber Estuary, and Tokyo Bay; though higher than Indian estuaries and Yangtze River Estuary (Hashimoto et al., 1999; De Wilde and De Bie, 2000; Zhang et al., 2010; Barnes and Upstill-Goddard, 2011; Rao and Sarma, 2013). The average N_2O flux from entire Pearl River Estuary was estimated to be 37 ± 15 μmol m^{-2} d^{-1}. This average flux density was similar to those exhibited in European estuaries, such as the Scheldt Estuary and Humber Estuary (De Wilde and De Bie, 2000; Barnes and Upstill-Goddard, 2011); though higher than most reported estuaries like Indian estuaries (Rao and Sarma, 2013). This was mainly due to higher DIN loadings and higher nitrification rates in the Pearl River Estuary.

The annual water–air N_2O emission of the Pearl River Estuary was estimated to be $(1.67 \pm 0.89) \times 10^9$ g N_2O yr^{-1} within an area of 2789 km^2. For comparison, this total emission from one anthropogenically impacted estuary was equivalent to the total emission from 19 European inner estuaries (1.35×10^9 g N_2O yr^{-1}), covering an area of ~1840 km^2 (Barnes and Upstill-Goddard, 2011). The previous estimates of N_2O emission in estuarine systems were mostly based on relative small European estuaries (Bange et al., 1996; Bange, 2006; Barnes and Upstill-Goddard, 2011). Clearly, with increasing anthropogenic stress, the Asian estuaries might hold an increasingly important role in budgeting the future global N_2O emission. Wide temporal and spatial variations of N_2O emission in Pearl River Estuary suggested that intensive monitoring is required; particularly for unexplored regions to obtain accurate contribution of estuaries to atmospheric N_2O.

5. Conclusions

Dissolved N_2O concentrations and water–air N_2O fluxes in the Pearl River Estuary showed wide spatiotemporal variation. A wide range of N_2O saturation levels varied from ~100% to 3800%, with substantially higher N_2O and N_2O fluxes observed during spring and winter in Upper Estuaries than in summer. Annual water–air N_2O emission from the Pearl River Estuary was estimated to be 3.8×10^7 mol, equivalent to ~30% of CO_2 emission in terms of greenhouse effect. The weighted average annual emission of N_2O from the Pearl River Estuary amounts to $(1.67 \pm 0.89) \times 10^9$ g N_2O yr^{-1}, which was equivalent to the revised emission estimate from 19 European inner estuaries (1.35×10^9 g N_2O yr^{-1}).

Variations of N_2O in the Pearl River Estuary were influenced by multiple factors in the Upper Estuary. N_2O production was enhanced under high-DIN loading and high-oxygen depletion conditions. Strong nitrification largely contributed to the high N_2O production. In the Lower and Middle Estuaries, mixing with lower N_2O seawater along with water–air N_2O exchanges was responsible for the variability of N_2O concentrations. Further research on direct N_2O production rate measurements in the water column and sediments (especially in the upper estuarine zone) from nitrification and denitrification are required to concretely define the controlling mechanism of N_2O in the Pearl River Estuary. High spatial and temporal observations are mandatory to further reduce the uncertainty of N_2O emission estimation.

Acknowledgments

This research was supported by the National Natural Science Foundation of China (NSFC) through projects #41130857, 41361164001, and 91328202. We sincerely thank the captain and crew of Yue Dongguang 00589 for their assistance during the sampling cruises. Xianghui Guo, Chuanjun Du, Liguo Guo, Jinwen Liu, Xu Dong, and Xiao Huang helped during the sampling and data collection. We are especially grateful to three anonymous reviewers and associate editor, Dr. Ron Kiene, for their constructive comments that helped improve the manuscript considerably.

References

Abril, G., Riou, S.A., Etcheber, H., Frankignoulle, M., de Wit, R., Middelburg, J.J., 2000. Transient, tidal time-scale, nitrogen transformations in an estuarine turbidity maximum-fluid mud system (the Gironde, south-west France). Estuar. Coast. Shelf Sci. 50 (5), 703–715.

Bange, H.W., Rapsomanikis, S., Andreae, M.O., 1996. Nitrous oxide in coastal waters. Glob. Biogeochem. Cycles 10 (1), 197–207.

Bange, H.W., 2000. It's not a gas. Nature 408, 301–302.

Bange, H.W., 2006. Nitrous oxide and methane in European coastal waters. Estuar. Coast. Shelf Sci. 70 (3), 361–374.

Bange, H.W., 2008. Gaseous nitrogen compounds (NO, N_2O, N_2, NH_3) in the ocean. In: Capone, D.G., Bronk, D.A., Mulholland, M.R., Carpenter, E.J. (Eds.), Nitrogen in the Marine Environment, second ed. Elsevier, Amsterdam, pp. 51–94 (Chapter 2).

Barnes, J., Upstill-Goddard, R.C., 2011. N_2O seasonal distributions and air–sea exchange in UK estuaries: Implications for the tropospheric N_2O source from European coastal waters. J. Geophys. Res. 116, G01006. http://dx.doi.org/10.1029/2009JG001156.

Borges, A.V., Delille, B., Schiettecatte, L.S., Gazeau, F., Abril, G., Frankignoulle, M., 2004. Gas transfer velocities of CO_2 in three European estuaries (Randers Fjord, Scheldt, and Thames). Limnol. Oceanogr. 49 (5), 1630–1641.

Chen, C.T.A., Wang, S.L., Lu, X.X., Zhang, S.R., Lui, H.K., Tseng, H.C., Wang, B.J., Huang, H.I., 2008. Hydrogeochemistry and greenhouse gases of the Pearl River, its estuary and beyond. Quat. Int. 186, 79–90.

Chen, Y., Yuan, D.X., Li, Q.L., 2007. Determination of nitrous oxide in seawater by room temperature purge and trap-gas chromatography. Chin. J. Anal. Chem. 35 (6), 897–900 (in Chinese).

Codispoti, L.A., Brandes, J.A., Christensen, J.P., Devol, A.H., Naqvi, S.W.A., Paerl, H.W., Yoshinari, T., 2001. The oceanic fixed nitrogen and nitrous oxide budgets: moving targets as we enter the anthropocene? Sci. Mar. 65, 85–105.

Codispoti, L.A., 2010. Interesting times for marine N_2O. Science 327 (5971), 1339–1340.

Cohen, Y., Gordon, L.I., 1979. Nitrous oxide production in the ocean. J. Geophys. Res. Oceans 84 (C1), 347–353.

Dai, M., Guo, X., Zhai, W., Yuan, L., Wang, B., Wang, L., Cai, P., Tang, T., Cai, W.-J., 2006. Oxygen depletion in the upper reach of the Pearl River Estuary during a winter drought. Mar. Chem. 102 (1–2), 159–169.

Dai, M., Wang, L., Guo, X., Zhai, W., Li, Q., He, B., Kao, S.-J., 2008. Nitrification and inorganic nitrogen distribution in a large perturbed river/estuarine system: the Pearl River Estuary, China. Biogeosciences 5, 1227–1244.

Dai, M., Gan, J., Han, A., Kung, H.S., Yin, Z., 2014. Physical dynamics and biogeochemistry of the Pearl River plume. In: Bianchi, T.S., Allison, M.A., Cai, W. (Eds.), Biogeochemical Dynamics at Large River-Coastal Interfaces. Cambridge University Press, Cambridge, pp. 321–352 (Chapter 13).

de Bie, M.J.M., Middelburg, J.J., Starink, M., Laanbroek, H.J., 2002. Factors controlling nitrous oxide at the microbial community and estuarine scale. Mar. Ecol. Prog. Ser. 240, 1–9.

De Wilde, H.P.J., De Bie, M.J.M., 2000. Nitrous oxide in the Schelde Estuary: production by nitrification and emission to the atmosphere. Mar. Chem. 69 (3–4), 203–216.

Dong, L.F., Nedwell, D.B., Colbeck, I., Finch, J., 2004. Nitrous oxide emission from some English and Welsh rivers and estuaries. Water Air Soil Pollut. Focus 4 (6), 127–134.

Dore, J.E., Karl, D.M., 1996. Nitrification in the euphotic zone as a source for nitrite, nitrate, and nitrous oxide at station ALOHA. Limnol. Oceanogr. 41 (8), 1619–1628.

Elkins, J.W., Wofsy, S.C., McElroy, M.B., Kaplan, W.A., Kolb, C.E., 1978. Aquatic sources and sinks for nitrous oxide. Nature 275 (5681), 602–606.

Garnier, J., Cébron, A., Tallec, G., Billen, G., Sebilo, M., Martinez, A., 2006. Nitrogen behaviour and nitrous oxide emission in the tidal Seine River estuary (France) as influenced by human activities in the upstream watershed. Biogeochemistry 77 (3), 305–326.

Goreau, T.J., Kaplan, W.A., Wofsy, S.C., McElroy, M.B., Valois, F.W., Watson, S.W., 1980. Production of NO_2^- and N_2O by nitrifying bacteria at reduced concentrations of oxygen. Appl. Environ. Microbiol. 40 (3), 526–532.

Guo, X., Dai, M., Zhai, W., Cai, W.-J., Chen, B., 2009. CO_2 flux and seasonal variability in a large subtropical estuarine system, the Pearl River Estuary, China. J. Geophys. Res. 114, G03013. http://dx.doi.org/10.1029/2008JG000905.

Harley, J.F., Carvalho, L., Dudley, B., Heal, K.V., Rees, R.M., Skiba, U., 2015. Spatial and seasonal fluxes of the greenhouse gases N_2O, CO_2 and CH_4 in a UK macrotidal estuary. Estuar. Coast. Shelf Sci. 153, 62–73.

Hashimoto, S., Gojo, K., Hikota, S., Sendai, N., Otsuki, A., 1999. Nitrous oxide emissions from coastal waters in Tokyo Bay. Mar. Environ. Res. 47 (3), 213–223.

He, B., Dai, M., Zhai, W., Wang, L., Wang, K., Chen, J., Lin, J., Han, A., Xu, Y., 2010. Distribution, degradation and dynamics of dissolved organic carbon and its major compound classes in the Pearl River estuary, China. Mar. Chem. 119 (1–4), 52–64.

He, B., Dai, M., Zhai, W., Guo, X., Wang, L., 2014. Hypoxia in the upper reaches of the Pearl River Estuary and its maintenance mechanisms: a synthesis based on multiple year observations during 2000–2008. Mar. Chem. 167, 13–24.

IPCC, 2007. Summary for Policymakers. In: Solomon, S., Qin, D., Manning, M., Chen, Z., Marquis, M., Averyt, K.B., Tignor, M., Miller, H.L. (Eds.), Climate Change, 2007: The Physical Science Basis. Contribution of Working Group I to the Fourth Assessment Report of the Intergovernmental Panel on Climate Change. Cambridge University Press, Cambridge, United Kingdom, and New York, NY, USA, pp. 2–18.

Kim, I.-N., Lee, K., Bange, H.W., Macdonald, A.M., 2013. Interannual variation in summer N_2O concentration in the hypoxic region of the northern gulf of Mexico, 1985–2007. Biogeosciences 10, 6783–6792.

Löscher, C.R., Kock, A., Könneke, M., LaRoche, J., Bange, H.W., Schmitz, R.A., 2012. Production of oceanic nitrous oxide by ammonia-oxidizing archaea. Biogeosciences 9 (7), 2419–2429.
McElroy, M.B., Elkins, J.W., Wofsy, S.C., Kolb, C.E., Duran, A.P., Kaplan, W.A., 1978. Production and release of N_2O from the Potomac Estuary. Limnol. Oceanogr. 23 (6), 1168–1182.
Middelburg, J.J., Nieuwenhuize, J., 2000. Uptake of dissolved inorganic nitrogen in turbid, tidal estuaries. Mar. Ecol. Prog. Ser. 192, 79–88. http://dx.doi.org/10.3354/meps192079.
Naqvi, S.W.A., Jayakumar, D.A., Narvekar, P.V., Naik, H., Sarma, V.V.S.S., D'Souza, W., Joseph, S., George, M.D., 2000. Increased marine production of N_2O due to intensifying anoxia on the Indian continental shelf. Nature 408, 346–349.
Naqvi, S.W.A., Bange, H.W., Farías, L., Monteiro, P.M.S., Scranton, M.I., Zhang, J., 2010. Marine hypoxia/anoxia as a source of CH_4 and N_2O. Biogeosciences 7, 2159–2190.
Nevison, C., Butler, J.H., Elkins, J.W., 2003. Global distribution of N_2O and the ΔN_2O-AOU yield in the subsurface ocean. Glob. Biogeochem. Cycles 17 (4), 1119. http://dx.doi.org/10.1029/2003GB002068.
Pai, S.-C., Tsau, Y.-J., Yang, T.-I., 2001. pH and buffering capacity problems involved in the determination of ammonia in saline water using the indophenol blue spectrophotometric method. Anal. Chim. Acta 434 (2), 209–216.
Patra, P.K., Lal, S., Venkataramani, S., De Sousa, S.N., Sarma, V.V.S.S., Sardesai, S., 1999. Seasonal and spatial variability in N_2O distribution in the Arabian Sea. Deep-Sea Res. I 46 (3), 529–543.
Rajkumar, A.N., Barnes, J., Ramesh, R., Purvaja, R., Upstill-Goddard, R.C., 2008. Methane and nitrous oxide fluxes in the polluted Adyar River and estuary, SE India. Mar. Pollut. Bull. 56 (12), 2043–2051.
Ravishankara, A.R., Daniel, J.S., Portmann, R.W., 2009. Nitrous oxide (N_2O): the dominant ozone-depleting substance emitted in the 21st century. Science 326 (5949), 123–125.
Rao, G.D., Sarma, V.V.S.S., 2013. Contribution of N_2O emissions to the atmosphere from Indian monsoonal estuaries. Tellus B 65.
Seitzinger, S.P., Kroeze, C., Styles, R.V., 2000. Global distribution of N_2O emissions from aquatic systems: natural emissions and anthropogenic effects. Chemosphere Global Change Sci. 2 (3), 267–279.
Walter, S., Bange, H.W., Breitenbach, U., Wallace, D.W., 2006. Nitrous oxide in the North Atlantic Ocean. Biogeosciences 3, 607–619.
Wong, M.H., Cheung, K.C., 2000. Pearl River Estuary and Mirs Bay, South China. In: Dupra, V., et al. (Eds.), Estuarine Systems of the South China Sea Region: Carbon, Nitrogen and Phosphorus Fluxes, LOICZ Reports and Studies Vol. 14. LOICZ, Texel, Netherlands, pp. 7–15.
Wanninkhof, R.I.K., 1992. Relationship between wind speed and gas exchange over the ocean. J. Geophys. Res. 97 (C5), 7373–7382.
Weiss, R.F., Price, B.A., 1980. Nitrous oxide solubility in water and seawater. Mar. Chem. 8 (4), 347–359.
Wu, J.Z., Chen, N.W., Hong, H.S., Lu, T., Wang, L.J., Chen, Z.H., 2013. Direct measurement of dissolved N_2 and denitrification along a subtropical river-estuary gradient, China. Mar. Pollut. Bull. 66 (1), 125–134.
Xu, J.R., Wang, Y.S., Wang, Q.J., Yin, J.P., 2005. Nitrous oxide concentration and nitrification and denitrification in Zhujiang River Estuary, China. Acta Oceanol. Sin. 24 (3), 122–130.
Yamagishi, H., Westley, M.B., Popp, B.N., Toyoda, S., Yoshida, N., Watanabe, S., Koba, K., Yamanaka, Y., 2007. Role of nitrification and denitrification on the nitrous oxide cycle in the eastern tropical North Pacific and Gulf of California. J. Geophys. Res. 112, G02015. http://dx.doi.org/10.1029/2006JG000227.
Yoshinari, T., Altabet, M.A., Naqvi, S.W.A., Codispoti, L., Jayakumar, A., Kuhland, M., Devol, A., 1997. Nitrogen and oxygen isotopic composition of N_2O from suboxic waters of the eastern tropical North Pacific and the Arabian Sea — measurement by continuous-flow isotope-ratio monitoring. Mar. Chem. 56 (3–4), 253–264.
Zhai, W.D., Dai, M.H., Cai, W.J., Wang, Y.C., Wang, Z.H., 2005. High partial pressure of CO_2 and its maintaining mechanism in a subtropical estuary: the Pearl River Estuary, China. Mar. Chem. 93 (1), 21–32.
Zhang, G.L., Zhang, J., Liu, S.M., Ren, J.L., Zhao, Y.C., 2010. Nitrous oxide in the Changjiang (Yangtze River) Estuary and its adjacent marine area: riverine input, sediment release and atmospheric fluxes. Biogeosciences 7, 3505–3516.